nature portfolio

Peer Review File

A coupled atmosphere-ocean source mechanism was a predictor of the 2022 Tonga volcanic tsunami

Corresponding Author: Dr Y. Tony song

Attachments originally supplied by the reviewers can be found at the end of this file, in order by reviewer number and revision

Version 0:

Decision Letter:

** Please ensure you delete the link to your author home page in this e-mail if you wish to forward it to your coauthors **

Dear Dr Song,

Your manuscript titled "Shocked atmosphere-ocean interplay reveals volcanic tsunami origin and predictive insight" has now been seen by 2 reviewers, whose comments are appended below. You will see that they find your work of some potential interest. However, they have raised quite substantial concerns that must be addressed. In light of these comments, we cannot accept the manuscript for publication, but would be interested in considering a revised version that fully addresses these serious concerns.

Please double check all reviewers' comments, following these two thresholds, which will be verified during the next review iteration:
1) please decide to use or not Krakatau as a reference case, and if so please provide appropriate and deep comparison, otherwise please just focus on Hunga Tonga;
2) please provide appropriate references for the source of parameters you used in the model. Such parameters (e.g., crater dimensions, etc...) should come from measurements or from scientific papers as references.

We hope you will find the reviewers' comments useful as you decide how to proceed. Should additional work allow you to address these criticisms, we would be happy to look at a substantially revised manuscript. If you choose to take up this option, please either highlight all changes in the manuscript text file, or provide a list of the changes to the manuscript with your responses to the reviewers.

When resubmitting, please provide a point-by-point response to the reviewers' comments. Please submit your responses as a separate file, distinct from your cover letter where you can add responses to the Editors' comments that you do not want to be made available to the reviewers. Word files are preferred.

Important: The response to reviewers must not include any figures, tables or graphs. If you wish to respond to the reviewer reports with additional data in one of these formats, please add them to the main article or Supplementary Information, and refer to them in the rebuttal. Due to current technical limitations, any figures, tables, or graphs embedded in your rebuttal will not be included in the peer review file, if published.

Please bear in mind that we will be reluctant to approach the reviewers again in the absence of substantial revisions.

If the revision process takes significantly longer than three months, we will be happy to reconsider your paper at a later date, as long as nothing similar has been accepted for publication at Communications Earth & Environment or published elsewhere in the meantime.

We are committed to providing a fair and constructive peer-review process. Please do not hesitate to contact us if you wish to discuss the revision in more detail.

Please use the following link to submit your revised manuscript, point-by-point response to the reviewers' comments with a list of your changes to the manuscript text (which should be in a separate document to any cover letter), a tracked-changes version of the manuscript (as a PDF file) and any completed checklist:

Link Redacted

** This url links to your confidential home page and associated information about manuscripts you may have submitted or be reviewing for us. If you wish to forward this email to co-authors, please delete the link to your homepage first **

Please do not hesitate to contact us if you have any questions or would like to discuss the required revisions further. Thank you for the opportunity to review your work.

Best regards,

Domenico M. Doronzo, PhD
Editorial Board Member
Communications Earth & Environment
orcid.org/0000-0002-6866-8870

Carolina Ortiz Guerrero, PhD
Associate Editor
Communications Earth & Environment

EDITORIAL POLICIES AND FORMAT

If you decide to resubmit your paper, please ensure that your manuscript complies with our editorial policies and complete and upload the checklist below as a Related Manuscript file type with the revised article:

Editorial Policy Policy requirements
(Download the link to your computer as a PDF.)

For Manuscripts that fall into the following fields:
• Behavioural and social science
• Ecological, evolutionary & environmental sciences
• Life sciences
An updated and completed version of our Reporting Summary must be uploaded with the revised manuscript
You can download the form here:
https://www.nature.com/documents/nr-reporting-summary.zip

For your information, you can find some guidance regarding format requirements summarized on the following checklist:
(https://www.nature.com/documents/commsj-phys-style-formatting-checklist-article.pdf) and formatting guide
(https://www.nature.com/documents/commsj-phys-style-formatting-guide-accept.pdf).

REVIEWER COMMENTS:

Reviewer #1 (Remarks to the Author):

The authors investigated the 2022 Hunga Tonga – Hinga Ha'apai tsunami resulting from the interaction between the air pressure created by the eruption and the ocean, by using an integrated ocean-atmosphere model. The results were validated from tide gauges, pressure gauges and satellite altimetry. I think the work has potential to be considered for publication, however, there are several major concerns that need to be addressed. The main points are reported below:

Major points:
• The title seems to be general in nature and potentially applicable to all volcanoes in similar shallow settings, however, the work proposed here only refers to HTHH and vaguely to Krakatau, with no further tests on other volcanoes. It should be reflected in the tile that was only for one case study: HTHH.

• The rationale behind the inclusion of some text on the 2018 Krakatau event is not clear nor contextualised. Was that event also entirely resulting from air-ocean interactions? It is not really investigated in the paper and seems out of context. If the intent of the authors was to argue that the 2018 Krakatau tsunami had a completely different origin mechanism than previously hypothesised, then at the moment it has just a speculative nature.

• Some of the parameters used for the model (crater diameter and crater depth) are approximative and retrieved (from my understanding) from a newspaper article (https://www.abc.net.au/news/2022-11-21/sea-floor-map-reveals-huge-cavity-left-behind-by-tonga-volcano/101674708). Research articles should be used for this purpose.

• The model shown in fig. 2 should be explained more clearly. There are several points that made me raise some questions (see various comments in the annotated pdf).

• The discussions lack any possible contribution, even if minor, of other tsunami source mechanisms. For example, the bathymetry they use shows clear landsliding from the rim within the caldera (Fig. S1).

See annotated pdf for minor and major comments in detail.

Dr Andrea Verolino

Reviewer #2 (Remarks to the Author):

Recommendation to the manuscript background information
Certainly! Here are some suggestions for revising the background information section of the manuscript.
1. Contextual Framework: Provide a concise overview of the current state of knowledge regarding volcanic tsunamis, highlighting key challenges and gaps in understanding the mechanisms that trigger volcanic tsunamis. Emphasize the difficulty in accurately predicting their occurrence and impact on coastal communities.
2. Historical Perspective: Briefly discuss significant historical events involving volcanic tsunamis, such as documented cases and their impact, including the Krakatau eruption of 1883 and more recent incidents (2018 Anak Krakatau, Pakoksung et al, 2019), to illustrate the destructive potential and variability of volcanic tsunamis.
3. Novel Research Question or Hypothesis: Clearly state the specific research question or hypothesis that your study is addressing. Explain how this query addresses a gap in the current understanding of volcanic tsunami mechanisms or predictive capabilities.
4. Unique Methodological Approach: Describe the innovative methodology or approach utilized in the study, such as the integration of an atmosphere-ocean model, a unique use of satellite altimetry data, or a creative application of air-pressure sensors for tsunami prediction.
5. Prior Research: Summarize previous studies and hypotheses related to volcanic tsunami generation mechanisms. Mention existing models or theories (without going into excessive detail) to provide context for how your study builds upon or challenges these previous findings.
6. Importance of Air-Pressure Waves: Introduce air-pressure waves, such as the "lamb wave," in understanding volcanic tsunami dynamics. Discuss the importance of studying air-pressure waves for enhancing early warning systems and disaster preparedness strategies.
7. Study Objectives: Clearly outline the study objectives in the background section to guide readers and manage expectations, such as discovering new predictors or enhancing predictive models for volcanic tsunamis.
8. Transition to Methodology: Transition smoothly from the background section to the methodology section by explaining how your study addresses gaps identified in prior research. This can help justify the need for your chosen methodology and research approach.
9. Conciseness and Focus: Keep the background section concise and focused, avoiding unnecessary details or tangential information that may distract from the manuscript's main objectives.
By revising the background information in this manner, you can provide a clear and informative context for your study on volcanic tsunamis. This will ensure that readers understand the significance of your research within the broader field of natural hazards and tsunami science.

Support Helpdesk.

Author Rebuttal letter: The author's response to these comments can be found at the end of this file.

Version 1:

Decision Letter:

** Please ensure you delete the link to your author home page in this e-mail if you wish to forward it to your coauthors **

Dear Dr Song,

Your revised manuscript titled "Coupled Atmosphere-Ocean Source Mechanism Reveals Predictors of the 2022 Tonga Volcanic Tsunami" has now been seen by our original reviewers, whose comments appear below. In light of their advice we are delighted to say that we are happy, in principle, to publish a suitably revised version in Communications Earth & Environment.

We therefore invite you to revise your paper one last time to address the remaining concerns of our reviewers. At the same time we ask that you edit your manuscript to comply with our format requirements and to maximise the accessibility and therefore the impact of your work.

EDITORIAL REQUESTS:

Please review our specific editorial comments and requests regarding your manuscript in the attached "Editorial Requests Table".

*****Please take care to match our formatting and policy requirements. We will check revised manuscript and return manuscripts that do not comply. Such requests will lead to delays. *****

Please outline your response to each request in the right hand column. Please upload the completed table with your manuscript files as a Related Manuscript file.

If you have any questions or concerns about any of our requests, please do not hesitate to contact me.

SUBMISSION INFORMATION:

In order to accept your paper, we require the files listed at the end of the Editorial Requests Table; the list of required files is also available at https://www.nature.com/documents/commsj-file-checklist.pdf .

OPEN ACCESS:

Communications Earth & Environment is a fully open access journal. Articles are made freely accessible on publication. For further information about article processing charges, open access funding, and advice and support from Nature Research, please visit https://www.nature.com/commsenv/open-access

At acceptance, you will be provided with instructions for completing the open access licence agreement on behalf of all authors. This grants us the necessary permissions to publish your paper. Additionally, you will be asked to declare that all required third party permissions have been obtained, and to provide billing information in order to pay the article-processing charge (APC).

Please use the following link to submit the above items:
Link Redacted
** This url links to your confidential home page and associated information about manuscripts you may have submitted or be reviewing for us. If you wish to forward this email to co-authors, please delete the link to your homepage first **

We hope to hear from you within two weeks; please let us know if you need more time.

Best regards,

Carolina Ortiz Guerrero, Ph.D.
Associate Editor
Communications Earth & Environment

REVIEWERS' COMMENTS:

Reviewer #1 (Remarks to the Author):

The main concerns I previously raised have been resolved, and the manuscript has significantly improved.

Reviewer #2 (Remarks to the Author):

Thank you very much to address all my comments, and your manuscript could be published in the journal.

Shocked atmosphere-ocean interplay reveals volcanic tsunami origin and predictive insight

Authors: Y. Tony Song[1*], Philip S. Callahan[1], Jean-Damien M. Desjonqueres[1], Severine Fournier[1] and Josh K. Willis[1]

Affiliations:
[1]Jet Propulsion Laboratory, California Institute of Technology, Pasadena, CA, 91109

*Corresponding author. Email: Tony.Song@jpl.nasa.gov

ABSTRACT

Volcanic tsunamis pose significant threats to nearby coastal communities. Despite extensive research, the mechanism behind tsunami generation remains unclear and the ability to forecast a destructive tsunami has proven elusive. Here we present novel findings derived from the 2022 Tonga volcanic incident, showing that the leading air-pressure wave holds promise as a key predictor of tsunami behavior. We constructed an integrated atmosphere-ocean model to explain the underlying mechanism and gathered satellite altimetry data for validation. In contrast to prior hypotheses[1-3], our results reveal that (1) the eruption process emerges as the pivotal factor governing both the air-pressure and tsunami dynamics; and (2) the crater size controls the volcanic ejecta to produce the air-pressure, and an equivalent water volume to power the tsunami. This study highlights the pivotal role of atmosphere-ocean interplay in generating volcanic tsunamis and advocates for incorporating air-pressure sensors into early warning systems.

The Hunga-Tonga Hunga-Haʻapai (HTHH) volcano, situated at 20.546°S and 175.390°W, approximately 65 km northwest of Tongatapu, Tonga, commenced its eruption at 4:07 UTC on January 15, 2022[4] (Fig. **1a-b**). NASA satellite imagery indicated intermittent eruption activity lasting for hours[5-7]. Seismometers recorded eruptions, equivalent to a 5.8-magnitude earthquake (https://earthquake.usgs.gov/earthquakes/eventpage/us7000gc8r/executive). The eruptions generated global air-pressure waves, detected circulating the planet multiple times[8]. Swift-traveling oceanic waves triggered tsunami alerts across the Pacific Ocean, resulting in minor impacts in distant areas[9-11]. Near the volcano, however, the eruption was destructive. The near-field tsunami killed three people and caused major destruction to many low-lying coastal communities on Tongatapu, ʻEua and the Haʻapai Group of Tonga. The resultant tsunami runups were up to 15 m at Mango Island and the inundation reached to 500 m as reported by the Tonga Geological Services[12]. The volcanic eruption, tsunami and ashfall caused an estimated US$90.4M in damages, the equivalent of approximately 18.5% of Tonga's Gross Domestic Product[13].

The most widely known volcanic eruption is the 1883 Krakatau event, which induced a 5.15 m tsunami, recorded by a Jakarta tide gauge[14]. The resulting devastation claimed over 36,000 lives, primarily through the subsequent tsunami, obliterating 300 villages around Indonesia's Sunda Strait between Java and Sumatra[15]. The 1883 volcanic eruption also generated a large atmospheric wave or lamb wave with significant oscillations in pressure over nine days as recorded by barometers in Europe and the United States[16,17]. On 22 December 2018, the Anak Krakatau ('Child of Krakatau') erupted anew and triggered a smaller yet still deadly tsunami. This event caused 431 fatalities, 7200 injuries, and displaced 46,646 individuals[18]. The eruption induced a Mw 5.1 earthquake in the regional seismic network[19].

Ever since the 1883 Krakatau incident, the formation of tsunamis via volcanic eruptions has remained a captivating enigma. Early studies suggested various formation mechanisms, including the submarine explosions, lateral blast, pyroclastic flows, large-scale collapse of the caldera, slope instability, volcano-tectonic earthquake, and shock waves[1-3]. The role of the air-pressure waves in the volcanic tsunamis has remained mysterious. In the 2018 Ana Krakatau event, satellite imaginary of land surface suggested that the eruption caused a flank failure. Modeling studies showed that it would need a volume of the flank failure in the range of 0.135–0.326 km^3 to reproduce the tsunami[20,21]. But a reconstruction of the flank failure from the satellite imagery provided a much smaller volume, about 0.1 km^3, in which 0.086~0.093 km^3 was submarine failure[22].

In the immediate aftermath of the 2022 Tonga volcanic incident, several of the mentioned hypotheses were employed to replicate the tsunami phenomenon[23-26]. For instance, Pakoksung et al[26] employed a prescribed sea-level perturbation characterized by a "V" profile as the initial condition for their tsunami model without the air-pressure waves. While the basic principle of tsunami generation necessitates the displacement of a substantial water volume, it's worth noting that the HTHH volcano, before the eruption, was positioned partially above sea level, with minimal water above the crater[5]. Adding to the enigma, recent seafloor surveys of the volcano have yielded no substantial indications of caldera or flank collapses[27]. The survey team discovered that the volcano's rim was remarkably intact, with no signs of a deep ocean explosion (Fig. S1).

The central question is how the volcanic eruption managed to trigger such a destructive tsunami with a relatively small amount of water present. Despite the discovery of the lamb wave over a century ago in 1881, its connection to volcanic tsunamis remains elusive. These uncertainties surrounding the genesis of tsunamis and air-pressure waves underscore the challenges in predicting volcanic tsunamis effectively to safeguard lives. In this study, we show that the volcanic eruption process serves as the pivotal factor governing both the air-pressure and tsunami dynamics. Both the air-pressure wave and the tsunami are intricately controlled by the size of the crater resulting from the eruption; therefore, the leading air-pressure wave has the predictive skill for the following tsunami.

Air-pressure and tsunami connection

We found that the air-pressure wave (Fig. **1c**), measured from the Tonga meteorological station, after converted into sea-level (by equation (1)-(2)), precedes the Tonga tide-gauge-recorded tsunami well in both strength and waveforms (Fig. **1d-e**). The air-pressure data originates from the Tonga Meteorological Office (Fig. S2), while the tide-gauge measurements at NuKu'alofa waterfront (nkfa) and Vuna Wharf (nkfa2) stations were sourced from https://www.ioc-sealevelmonitoring.org/ (Fig. S3). Notably, the three instances of low air pressure correspond closely to the respective heights of the tsunami, recorded by the tide-gauges. The three pressure lows indicate three major eruptions at HTHH[26]. The correlation exhibits exceptional accuracy in the first wave (Fig. S4), but less so in subsequent waves due to the lingering effects of the first and largest wave within the vicinity of Tonga's islands and harbors. When it comes to tsunami warnings, the primary concern is the first and largest wave. The nkfa tide gauge experienced malfunctioning at 5:25 UTC, but still captured the two important waves, which confirms the correlation between the air-pressure wave and the tsunami.

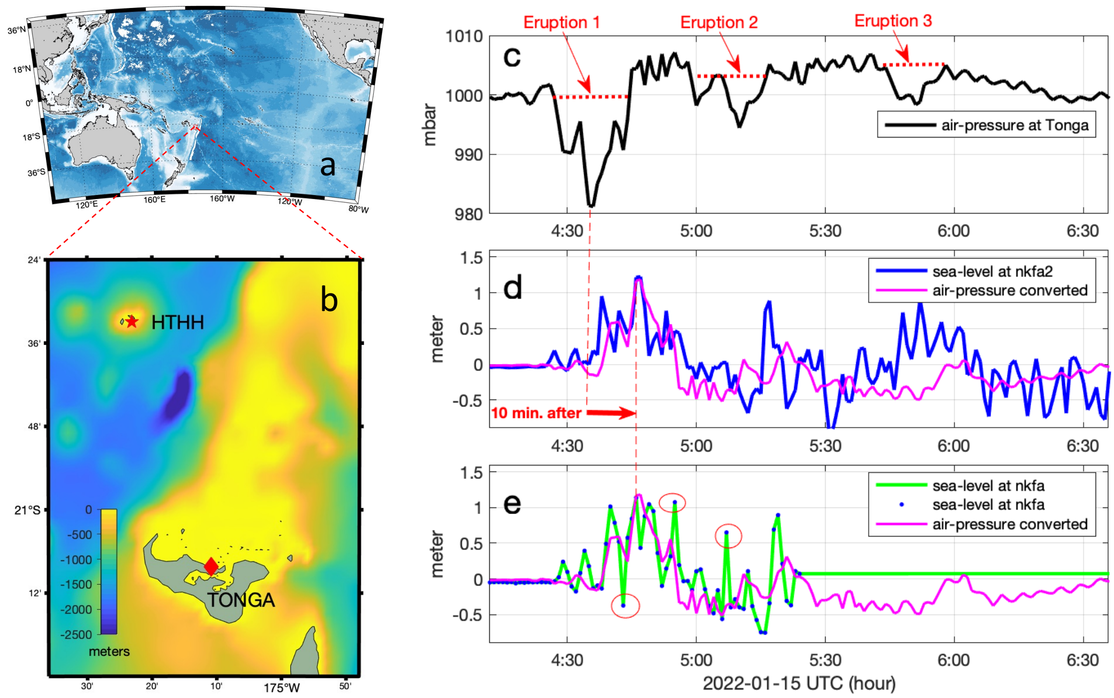

Fig. 1. Air-pressure and tide-gauge in Tonga. a. Location of the HTHH volcano. **b**. Zoom of the local bathymetry, in which the red-diamond indicates the Tonga tide-gauge locations. **c**. Air-pressure data from Tong with three distinct troughs, indicating three significant eruption cycles commencing at 4:26, 5:01, and 5:46. Each last approximately 20 minutes. **d**. Tide-gauge data from Tonga (nkfa2 station), compared with air-pressure converted sea-level (magenta, by equation (1)-(2)). **e.** Tide-gauge data from Tonga

(nkfa station), compared with air-pressure converted sea-level (magenta, by equation (1)-(2)). Note that the nkfa tide gauge (green) experienced a malfunction at 5:25, and the red circles indicate data points that fall outside the expected range, likely attributed to sensor issues.

The correlation is established as the following. First, we converted the air-pressure (black line in Fig. **1c**) into sea-level anomaly (magenta in Fig. **1d-e**) based on the principle of *inverted barometer* (*IB*) effect, i.e., an increase in air pressure (p_a) of 1 mbar corresponds to a surface depression of approximately 1 cm. Mathematically, the effect of the air pressure on the sea level can be written as $\eta^{ib} = -p_a/g\rho$, where ρ is the water density, and g is the gravity coefficient. This formula converts the atmospheric pressure anomaly into the thickness of water. We then convert the thickness of water into tsunami with the empirical tsunami runup formula at the Tonga coast[28]:

$$\eta(t+\tau) = -(p_a(t)/g\rho)R_f \qquad (1)$$

Here R_f is the empirical runup factor, t is the time, and $\tau = d/v_o - d/v_a$ is the lead-time of the air-pressure wave over the tsunami at the measurement location, in which d is the distance from the volcano, v_a and v_o are the travel speed of the air-pressure wave and the tsunami, respectively. We have used the calibrated formulation based on coastal measurements[29]:

$$R_f = 1.29\left(\tan(\alpha)\sqrt{L_o/H_o}\right)^{0.72} \qquad (2)$$

Here L_o is the wavelength, H_o is the significant tsunami height, and α is the slope angle. Their values are 40 km, 1.2 m, and 3.6 degrees in the Tonga case, similar to those used in previous studies[28, 29].

Note that air-pressure waves travel in the atmosphere with negligible effect by the coast and land. Differently, tsunami becomes slower and increase its height toward the coast. Both air-pressure and tsunami travel speed can be estimated precisely as the atmosphere and ocean depth are known[30]. Tonga is located about 65 km from the volcano. The speed of the air-pressure wave is about 330 m/s, traveling in the atmosphere with an averaged depth of 11.2 km. The speed of the tsunami is about 82 m/s in the near field, based on bathymetry data that has an average depth of 680 m from the volcano to Tonga. The arrival time was 3 minutes for the air-pressure wave and 13 minutes for the tsunami, respectively. The air-pressure lead-time is about 10 minutes, which is used in equation (1)-(2), aligning well with the actual data observed in Tonga.

Atmosphere-ocean interplay

To explain the physical connections between the air-pressure wave and the tsunami, we constructed an integrated atmosphere-ocean model based on the open-source code of the Regional Ocean Modeling System (ROMS), which is available online (www.myroms.org). ROMS is a full hydrodynamic ocean general circulation model, widely used in the oceanography community for various applications[31,32]. For tsunami simulation, the shallow-water equation module with a constant water density is used, which is like the widely used tsunami model of Satake[33]. In this study, we used 12-vertical levels for the water column—a similar setting used in previous studies of the 2004 Indian Ocean tsunami and the 2011 Japan tsunami[34,35].

For the atmospheric pressure waves (or lamb waves), we used the same ROMS model, but replaced the ocean depth (bathymetry) with the atmosphere depth. Following Amores et al[36], the atmosphere depth can be derived by

$$H_A = \frac{\gamma \cdot R \cdot T}{\mathrm{M} \cdot \mathrm{g}}, \qquad (3)$$

where $\gamma = 1.4$ is the nondimensional ratio of specific heat of air corresponding to the range of atmospheric temperatures, $R = 8314.36$ J/kmol/K is the universal gas constant, T is the absolute temperature, with a mean value of 273.15, and $M = 28.966$ kg/kmol is the molecular mass for dry air. The mean atmosphere depth is about 11189.24 m. The atmosphere pressure is converted into equivalent water thickness by a factor of $1/g\rho$, meaning 1 millibar corresponds to 1 centimeter of water thickness.

We initialized the atmosphere and ocean model by the same sequence of eruption process, but with an opposite orientation of initial velocity field (method 1), as schematically shown in Figure **2a**. Note that both the atmosphere and ocean models are the depth-averaged shallow-water-equation model. Their progressive variables are the surface elevation η and the depth-averaged velocity (U, V), representing the air-pressure wave and depth-averaged air velocity in the atmosphere, as well as the sea-level (or tsunami) and depth-averaged ocean velocity in the ocean, respectively. The air-pressure wave and the tsunami can be initialized either by a perturbation of the surface η or the velocity (U, V)[37]. In our case, the atmosphere model is initialized by a depth-averaged air velocity away from the crater, while the tsunami model is initialized by a depth-averaged ocean velocity toward the crater, respectively (Fig. **2b-c**).

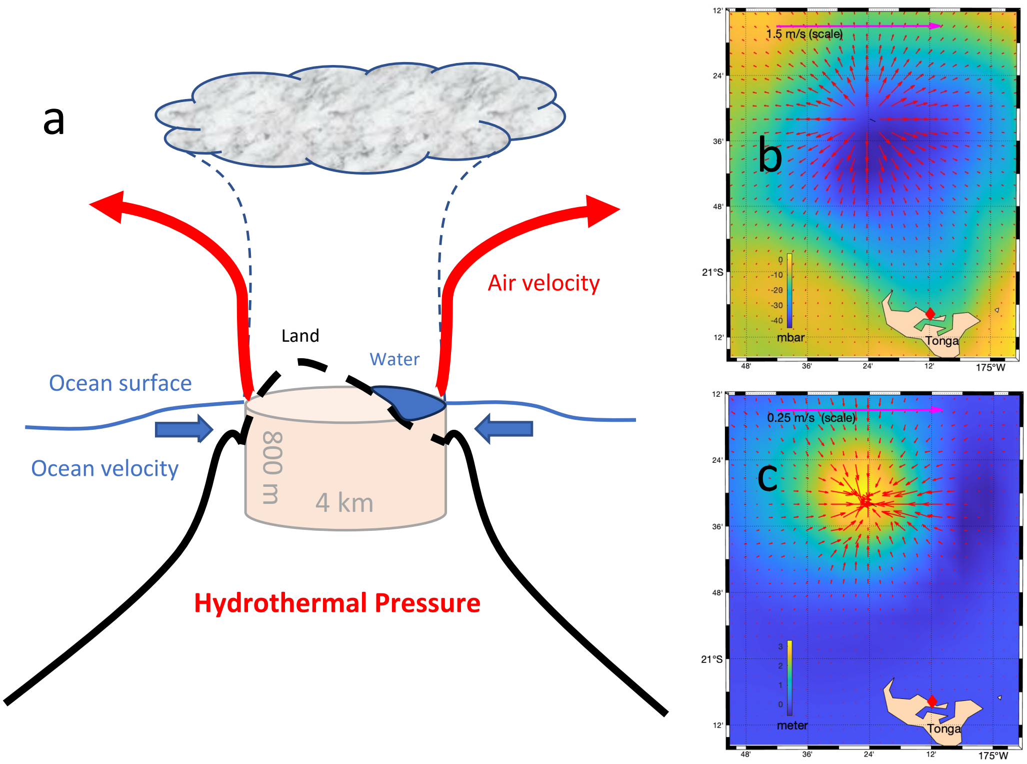

Fig. 2. Genesis of lamb wave and tsunami. a. Schematics of the atmosphere-ocean interplay during the volcanic eruptions. The brown cylinder with a diameter of 4 km and a depth of 800 m presents the crater, caused by volcanic ejecta of waters, gases, and magma to the atmosphere. The red arrow indicates atmosphere gained mass and

expansion of air, which triggers the lamb wave; while the blue arrows indicate water velocity to fill the water cavity in the ocean, which generates the tsunami. **b.** Depth-averaged air velocity depicted by the red arrows, illustrating the lateral blast as air radiates away from the crater. The background color corresponds to the air pressure anomaly one minute after initialization. **c.** Depth-averaged water velocity represented by the red arrows, showcasing the movement of ocean water toward the crater. The background color reflects the sea level one minute after initialization.

In the atmosphere model, the outward initial velocity field represents the explosion of air due to the eruption, which is consistent with satellite images, showing the eruption expanded hundreds of kilometers in the sky[5~7]. The initial conditions represent three sequences of volcanic eruptions for a period of 20 minutes with strength reduced by a half in each period, as suggested by the Tonga air-pressure data. Air pressure caused by volcano eruption is primarily a low-pressure system at Earth's surface—the atmospheric base. The atmospheric model generates a negative air-pressure anomaly as shown by the background color with a minimum of 35 mbar (Fig. **2b**). This air-pressure *IB* is applied to ocean model as the sea-surface condition.

In the ocean model, the initial velocity field is an inward flow field toward the crater, opposite to the initial atmosphere field, representing the movement of the ocean water to fill up the erupted cavity (Fig. **2c**). The atmospheric and oceanic initial conditions are implemented at the same time-sequence and resulted in an accumulated kinetic energy of 7.8×10^{15} Joule for the atmosphere and 3.5×10^{14} Joule for the ocean, respectively (method 1).

We run the two models in parallel, and sum their results as the total (atmospheric and oceanic) tsunami,

$$\eta^{A+O} = -\eta^{A} + \eta^{O} \quad (4)$$

Here, η is the total sea-level anomaly or tsunami, where A and O indicate the components of atmospheric and oceanic tsunami, respectively. The negative sign of the atmospheric component represents the inverse barometer (*IB*) effect, resulting in a sea-level depression when there is a positive air-pressure anomaly. Removing the negative sign, $\eta^{A} + \eta^{O}$ represents the total ocean bottom pressure, where η^{A} is the equivalent air-pressure measurements on land adjusted by $g\rho$.

Fig. **3** shows the simulated air-pressure wave and tsunami at the Tonga location, compared with the smoothed Tonga air-pressure and tide-gauge data to focus on the large features represented by the model. The model reproduced the data well in both strength and waveforms, suggesting that the correlation (Fig. S4) between the air-pressure wave and the tsunami have fundamental physical connections, at least in the near-field.

The model results were further validated by far-field observations, including the Deep-ocean Assessment and Reporting of Tsunamis (DART) data, air-pressure measurements on land, and satellite altimetry data. The DART system measures the ocean bottom pressure[38], which has been converted to the equivalent of water thickness in meters (i.e., $\eta^{A} + \eta^{O}$). We compared our model results with the DART measurements, showing that the integrated atmosphere-ocean model represents the magnitude and speed of the tsunami well (Fig. S5). Specifically, they show two kinds of tsunamis: the atmospheric tsunami is traveling with the lamb wave speed of 330 m/s, as highlighted by the dashed-green line; while the oceanic tsunami is propagating at various speeds, depending on the water depth, in an average speed of 160 m/s. On the land, air pressure gauges are accessible. We conducted further comparisons of model air pressures (i.e., η^A) with extended data from surrounding islands, revealing consistent air pressure patterns (Fig. S6).

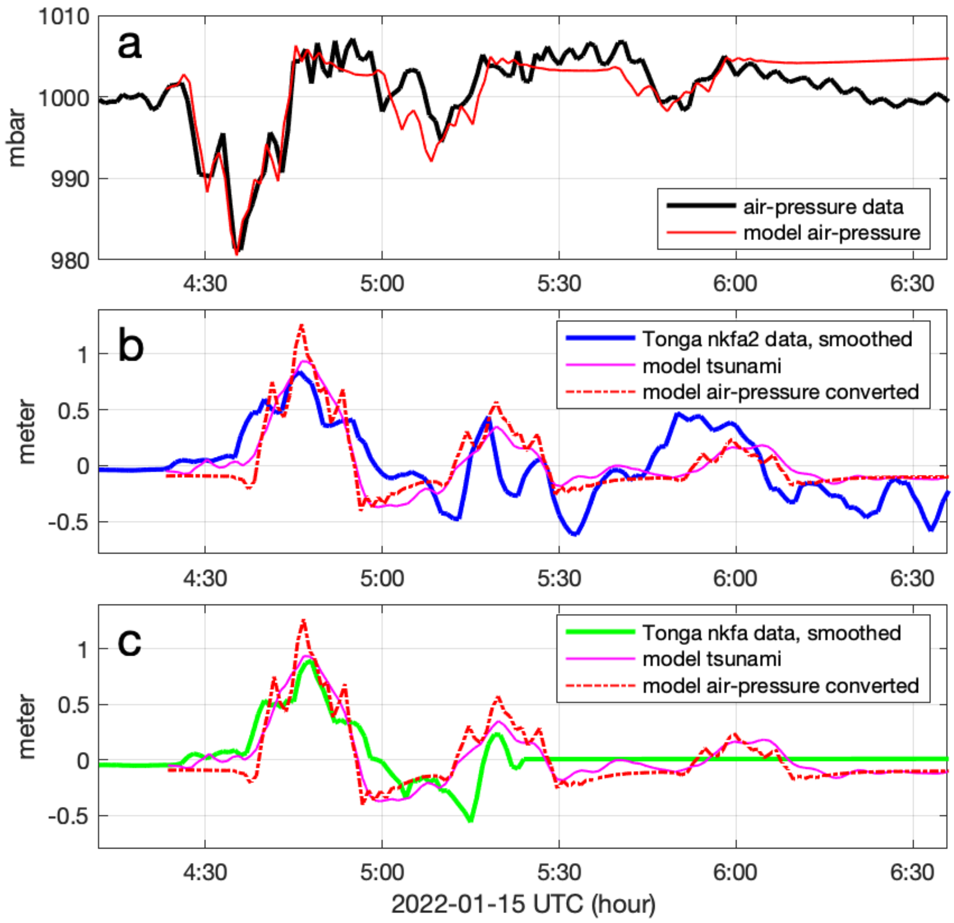

Fig. 3. Model air-pressure and tsunami, compared with Tonga data. a. Air pressure comparison. **b**. Sea level comparison at nkfa2. **c**. Sea level comparison at nkfa. Dash-lines are air-pressure converted sea-level by equation (1)-(2).

However, volcanic tsunamis have the effect of atmosphere pressure (i.e., $-\eta^A + \eta^O$). Surface observations are crucial evidence for elucidating the mysterious role of air-pressure waves. Previously, satellite altimetry has demonstrated its capability to measure earthquake tsunamis[35, 37]. Unlike DART and air-pressure gauges, satellite altimeters offer a synoptic view of the tsunami in the open ocean, often closer to the epicenter. The HTHH event was the first significant volcanic eruption to have occurred in the satellite era. We examined all possible satellite altimetry measurements that might have captured the surface displacement of the tsunamis, including the India-French satellite AltiKa (https://altika-saral.cnes.fr/en/SARAL/GP_mission.htm), and the Jason-3 and Sentinel-6 Michael Freilich (S6A) satellite (https://sealevel.jpl.nasa.gov/missions/overview-and-partners/). We processed the data to compare with the model by co-locating the satellite passes with the model in time and location (method 2 and Fig. S7). For the first time, we found that the satellite altimetry captured the tsunami on both near-filed and far-field locations. The AltiKa satellite observed the tsunami within locations between 19°S and 28°S during 29-38 minutes after the eruption, while the S6A and Jason-3 satellites, 30 seconds apart, measured the tsunami through the volcano center, 5 hours after the eruption (Fig. S8). Surprisingly, the tsunamis fell well within the range of typical ocean dynamic signals, suggesting that the destructive force of the volcanic tsunami might have diminished in these regions.

Genesis of lamb wave and volcanic tsunami

The primary evidence from the Tonga volcanic observations centers on the connection between the air-pressure wave (or lamb wave) and the tsunami, a connection previously unexplored. Our atmosphere-ocean model put forth a novel explanation for the interplay between the atmosphere and ocean in generating the Tonga volcanic tsunami and the lamb wave. In the atmosphere model, we employ the lateral blast mechanism—caused by the rapid expansion of air—to initiate the air pressure waves. This mechanism explains the satellite imagery showing the mushroom cloud in the sky during the eruptions. It is also corroborated by the wind data from the Tonga Met Office (Fig. S2(right)). The wind gust arrived in Tonga about 45 minutes after the eruption with a maximum speed of 40 m/s, suggesting the lateral movement of air by the eruption. Together, these lines of evidence consistently suggest a lateral forcing mechanism of hot air, resulting in the formation of a low-pressure center in the near-field (Fig. **1**) and resulting in a high-pressure anomaly of lamb wave extending to the far fields (Fig. S5-6)—a phenomenon unique to volcanic eruptions. This explanation sheds light on the mystery surrounding the generation of a lamb wave within an 11 km-depth atmosphere by a 4 km-sized volcano.

In the ocean, the situation becomes more intricate due to the formation of a water cavity during volcanic eruptions, ultimately resulting in an underwater crater. By the continuity principle of fluid flow, surrounding ocean waters must fill the water cavity, which would induce ocean mass movement necessary for the generation of the tsunami. Simultaneously, the large-scale low-pressure center above would raise the sea-level upward. This causes lateral water movement towards the crater, further enhancing the mechanism to trigger the tsunami. Eyewitness reports of sea-level recession preceding the tsunami along the Tonga coast[39] further corroborate this intricate atmosphere-ocean interplay, highlighting the initial movement of water towards the crater. This explanation sheds light on the puzzle of how volcanic eruptions, often occurring atop seamounts or partially above sea level, can trigger tsunamis despite the limited water volume present. In contrast to earthquake-triggered tsunamis, which involve large-scale movement at the deep ocean floor and exhibit transoceanic devastation potential[34, 40], volcanic tsunamis possess a distinct characteristic—they are exceptionally destructive in the near field but comparatively less damaging in the far field, despite their extensive reach. This distinction may be attributed to the surface forcing mechanism of atmosphere-ocean interplay, resembling a combined behavior of storm surges and earthquake-induced tsunamis.

Pressure sensors for early warning

The intrinsic and measurable correlation between air pressure waves and volcanic tsunamis presents a promising avenue for predicting volcanic tsunamis using air pressure sensors. Specifically, our research demonstrates that the mass ejected into the atmosphere during a volcanic eruption equals the mass lost in the ocean, establishing the basis for a quantitative and temporal link between air pressure waves and tsunamis. This relationship is governed by the intensity of the eruption and the size of the crater, while the air pressure wave is the front runner. In Figure **4a-b**, we computed the lead times of air pressure waves preceding tsunamis using the empirical equations (1)-(2) for both HTHH and Krakatau regions. Our analysis reveals that most residents reside within 30 to 60 km of the volcanoes, as indicated by the dash-line circles in both regions. The lead times are about 5 to 10 minutes between the inner and outer circles.

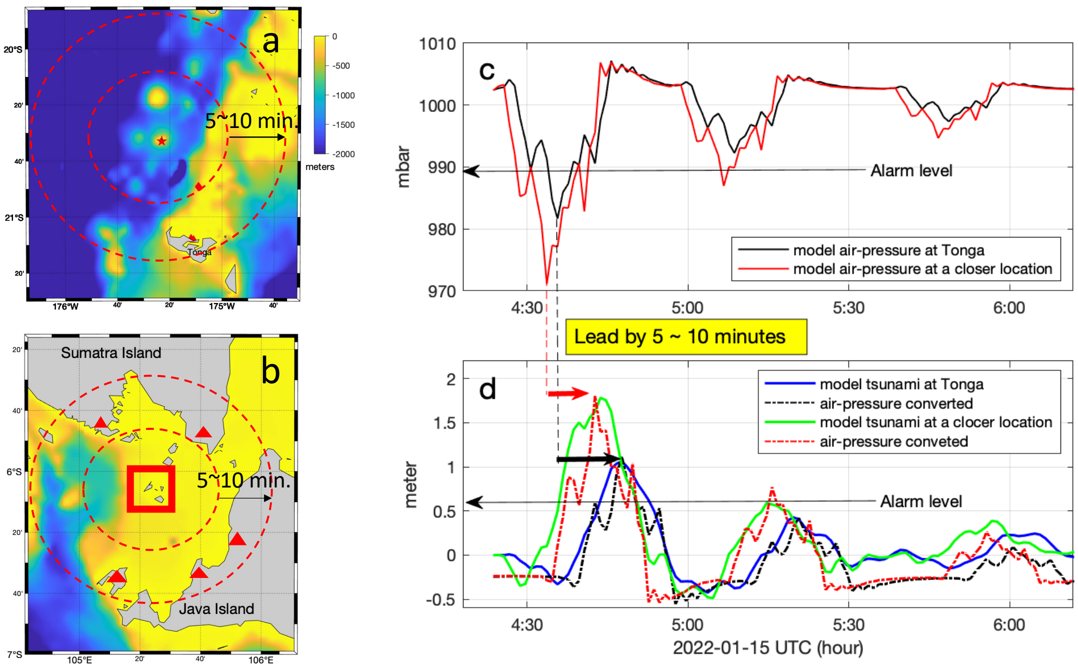

Fig. 4. Air-pressure leads tsunamis in the coupled atmosphere-ocean model. a. Lead-times around HTHH. **b.** Lead-times around Krakatau. The dash-line inner and outer circles highlight the lead-times of the air-pressure wave preceding the tsunami by 5 to 10 minutes. **c**. Model air pressures at Tonga (outer circle) and a closer location (inner circle). **d**. Model tsunami and air pressure converted sea-level by equations (1)-(2) at Tonga (outer circle) and a closer location (inner circle) near HTHH.

Due to the lack of co-located air-pressure and tsunami data from the Krakatau events, we directed our attention towards the Tonga region. Figure **4c-d** compares the model results of the air pressure and tsunami at the inner circle (30 km from the HTHH) with those at the outer circle (Tonga, located approximately 65 km from HTHH). The lead times generated by our model are consistent with the empirical calculations based on equations (1)-(2). Moreover, the magnitudes of the air pressure wave and subsequent tsunami within the inner circle nearly double those in the outer circle. This might explain the catastrophic outcomes in the incidents of 1883 and 2018, as numerous coastal settlements along the Indonesian Sunda region are situated within a 30-kilometer radius of the Krakatau volcanoes.

Given the similar geographical characteristics of the Tonga and Krakatau regions, deploying air pressure sensors across surrounding coastal communities is strongly recommended. These sensors could serve to monitor volcanic activity, validate future research findings, and establish a baseline threshold for calibration. Should a volcanic eruption generate an air pressure anomaly surpassing the designated threshold, such as 15 mbar, an alert or alarm system could be activated to promptly notify and safeguard coastal residents. Indeed, throughout history, the devastating impacts of volcanic tsunamis have been predominantly confined to the near field of the eruption epicenter. Satellite altimetry measurements have substantiated the confinement of the Tonga tsunami. Within the near-field perimeter, a lead time of approximately 5 to 10 minutes exists, providing a crucial window for evacuation measures.

Supplementary information

Any methods, additional references, source data, extended data, supplementary information, acknowledgements; details of author contributions and competing interests; and statements of data and code availability are available online.

Reference

1. Francis, P. W. The origin of the 1883 Krakatau tsunami, *J. Volcanol. Geotherm. Res*., **25**, 349-363 (1985). https://doi.org/10.1016/0377-0273(85)90021-6.
2. Paris R. Source mechanisms of volcanic tsunamis. *Phil. Trans. R. Soc*. **A** 373 (2015). http://dx.doi.org/10.1098/rsta.2014.0380.
3. Nomanbhoy, N. & Satake, K. Generation mechanism of tsunamis from the 1883 Krakatau eruption, *Geophys. Res. Letters* **22**, 509-512 (1995).
4. Donner, S., A. Steinberg, J. Lehr, C. Pilger, P. Hupe, P. Gaebler, J. O. Ross, E.P. S. Eibl, S. Heimann, D. Rebscher, T. Plenefisch, L. Ceranna, The January 2022 Hunga Volcano explosive eruption from the multi technological perspective of CTBT monitoring. *Geophys. J. Int*., **235**, 48-73 (2023). https://doi.org/10.1093/gji/ggad204.
5. NASA. Dramatic change at huga tonga-hunga ha'apai (2022). https://earthobservatory.nasa.gov/images/149367/dramatic-changes-at-hunga-tonga-hunga-haapai
6. Duncombe, J. The surprising reach of Tonga's giant atmospheric waves, *Eos* **103** (2022). https://doi.org/10.1029/2022EO220050
7. Lee, L. Tonga eruption made waves in Earth's ionosphere, *Eos*, **103**, 21 April (2022). https://doi.org/10.1029/2022EO220202
8. Wright, C.J. et al. Surface-to-space atmospheric waves from Hunga Tonga-Hunga Ha'apai eruption, https://doi.org/10.1038/s41586-022-05012-5 (2022).
9. Kubota, T., T. Saito, K. Nishid, Global fast-traveling tsunamis driven by atmospheric Lamb waves on the 2022 Tonga eruption, *Science* **377**, 91–94 (2022).
10. Imamura, F., A. Suppasri, I. Arikawa, A. Koshimura, K. Satake, Y. Tanioka, Preliminary Observations and Impact in Japan of the Tsunami Caused by the Tonga

Volcanic Eruption on January 15, 2022, *Pure Appl. Geophys*. **179**, 1549–1560 (2022). https://doi.org/10.1007/s00024-022-03058-0.

11. Tanioka, Y., Y. Yamanaka, T. Nakagaki, Characteristics of the deep sea tsunami excited offshore Japan due to the air wave from the 2022 Tonga eruption. *Earth, Planets and Space*, **74**(1), 1-7 (2022).
12. Borrero, J. C., S. Cronin, F. H. Latu'ila, P. Tukuafu, N. Heni, N. M. Tupou, T. Kula, O. Fa'anunu, C. Bosserelle, P. Lynett, L. Kong, Tsunami Runup and Inundation in Tonga from the January 2022 eruption of Hunga Volcano. *Pure and Applied Geophysics*, **180**, 1-22 (2023). https://doi.org/10.1007/s00024-022-03215-5
13. World Bank Assessment (2022). https://www.worldbank.org/en/news/press-release/2022/02/14/tonga-volcanic-eruption-and-tsunami-world-bank-disaster-assessment-report-estimates-damages-at-us-90m.
14. Pelinovsky, E., B. H. Choi, A. stromkov, L. Didenkulova, H._S. Kim, Analysis of tide-gauge records of the 1883 Krakatau tsunami, K. Satake (ed.), Tsunamis: Case Studies and Recent Developments, 57-78 (2005). Springer. Printer in Netherlands.
15. Bryant, T. Tsunamis, Cambridge University Press (2001).
16. Lamb, H. On the vibrations of an elastic sphere. *Proceedings of the London Mathematical Society*, **s**1-13 (1), 189-212 (1881). https://londmathsoc.onlinelibrary.wiley.com/doi/abs/10.1112/plms/s1-13.1.189
17. Simkin, T., R. S. Fiske, Krakatau 1983: the volcanic eruption and it effects. Washington, D.C.: Smithsonian Institute Press, (1983). Pp646.
18. BNPB (2019). Tsunami Selat Sunda. BNPB - National Disaster Management Agency. https://bnpb.go.id/berita/tsunami-selat-sunda.
19. Ye, L., H. Kanamori, L. Rivera, T. Lay, Y. Zhou, D. Sianipar, K. Satake, The 22 December 2018 tsunami from flank collapse of Anak Krakatau volcano during eruption, *Sci. Adv*. **6** (2020). eaaz1377.
20. Grilli, S. T., D. R. Tappin, S. Carey, S. F. L. Watt, S. N. War, A. R. Grilli, S. L. Engwell, C. Zhang, J. T. Kirby, L.Schambach, M. Muin, Modelling of the tsunami from the December 22, 2018 lateral collapse of Anak Krakatau volcano in the Sunda Straits, Indonesia. *Scientific Reports*, **9**(1), 1–13 (2019). https://doi.org/10.1038/s41598-019-48327-6.
21. Omira, R. & Ramalho, I. Evidence-Calibrated Numerical Model of December 22, 2018, Anak Krakatau Flank Collapse and Tsunami, *Pure Appl. Geophys*. **177**, 3059–3071 (2020). https://doi.org/10.1007/s00024-020-02532-x.

22. Williams, R., P. Rowley, M. C. Garthwaite, Reconstructing the Anak Krakatau flank collapse that caused the December 2018 Indonesian tsunami. *Geology*, **47**(10), 973–976 (2019). https://doi.org/10.1130/G46517.1.

23. Omira, R., R. S. Ramalho, J. Kim, P. J. Gonzalez, U. Kadri, J. M. Miranda, F. Carrilho, M. A. Baptista, Global Tonga tsunami explained by a fast-moving atmospheric source. *Nature* **609**, 734–740 (2022). https://doi.org/10.1038/s41586-022-04926-4

24. Lynett, P., M. McCann, Z. Zhou, W. Renteria, J. Borrero, D. Greer, O. Fa'anunu, C. Bosserelle, B. Jaffe, S. La Selle, A. Ritchie, A. Snyder, B. Nasr, J. Bott, N. Graehl, C. Synolakis, B. Ebrahimi, G. E. Cinar, Diverse tsunamigenesis triggered by the Hunga Tonga-Hunga Ha'apai eruption, *Nature*, vol 609 (2022). https://doi.org/10.1038/s41586-022-05170-6.

25. Purkis, S. J., S. W. Ward, N. M. Fitzpatrick, J. B. Garvin, D. Slayback, S. J. Cronin, M. Palaseanu-Lovejoy, A. Dempsey, The 2022 Hunga-Tonga megatsunami: Near-field simulation of a once-in-a-century event, *Sci. Adv*. **9**, eadf5493 (2023).

26. Pakoksung, K., A. Suppasri, F. Imamura, The near-field tsunami generated by the 15 January 2022 eruption of the Hunga Tonga-Hunga Ha'apai volcano and its impact on Tongatapu, Tonga. *Sci Rep.,* (2022). doi: 10.1038/s41598-022-19486-w.

27. Doman, M. & A. Palmer. The 'mind-blowing' sea floor changes caused by Tongan volcanic eruption (2022), https://www.abc.net.au/news/2022-11-21/sea-floor-map-reveals-huge-cavity-left-behind-by-tonga-volcano/101674708.

28. Park, H. & D. T. Cox, Empirical wave run-up formula for wave, storm surge and berm width, *Coastal Engineering* **115**, 67–78 (2016). http://dx.doi.org/10.1016/j.coastaleng.2015.10.006.

29. Paprotny, D., P. Andrzejewski, P. Terefenko, K. Furmanczyk, Application of Empirical Wave Run-Up Formulas to the Polish Baltic Sea Coast. *PLoS ONE* **9**(8) (2014). Doi: e105437. doi:10.1371/journal.pone.0105437.

30. Shokin, Y. I., L. B. Chubarov, V. A. Novikov, A. N. Sudakov (1987), Calculations of tsunami travel times in the Pacific Ocean (models, algorithms, techniques, results), *Science of Tsunami Hazards*, **5**(2), (1987).

31. Song, Y. T. & D. Haidvogel, A semi-implicit primitive equation ocean circulation model using a generalized topography-following coordinate system. *J. Comput. Phys.*, **115**, 228-244 (1994).

32. Shchepetkin, A. & J. C. McWilliams, The regional oceanic modelling system (ROMS): a split-explicit, free surface, topography-following-coordinate oceanic model. *Ocean Modelling*, **9**, 347–404 (2005).

33. Satake, K. Linear and nonlinear computations of the 1992 Nicaragua earthquake tsunami, *PAGEOPH*, 144, 455-470 (1995).

34. Song, Y. T., L.-L. Fu, V. Zlotnicki, C. Ji, V. Hjorleifsdottir, C.K. Shum, and Y. Yi, The role of horizontal impulses of the faulting continental slope in generating the 26 December 2004 Tsunami, *Ocean Modelling*, (2008). doi:10.1016/j.ocemod.2007.10.007.

35. Song, Y. T., I. Fukumori, C.K. Shum, and Yuchan Yi, Merging tsunamis of the 2011 Tohoku-Oki earthquake detected over the open ocean, *Geophys. Res. Lett*., (2012). doi:10.1029/2011GL050767.

36. Amores, A., S. Monserrat, M. Marcos, D. Argüeso, J. Villalonga, G. Jordà, D. Gomis, Numerical simulation of atmospheric Lamb waves generated by the 2022 Hunga-Tonga volcanic eruption. *Geophysical Research Letters*, **49** (2022). https://doi.org/10.1029/2022GL098240

37. Song, Y. T., C. Ji, L.-L. Fu, V. Zlotnicki, C.K. Shum, Y. Yi, and V. Hjorleifsdottir The 26 December 2004 Tsunami Source Estimated from Satellite Radar Altimetry and Seismic Waves, *Geophys. Res. Lett*., **23** (2005). doi:10.1029/2005GL023683.

38. NOAA NDBC: https://www.ndbc.noaa.gov/obs.shtml?lat=13&lon=-173&zoom=2&pgm=tsunami.

39. Lytton, C., D. Hawkins, M. Abbott, S. Tan, F. Hulley-jones, The day an underwater volcano almost wiped out a nation - *The Washington Post*. May 2023, https://apple.news/AKXWDUyOOTCq-NQCTtFBNfQ

40. Tanioka, Y. & K. Satake, Tsunami generation by horizontal displacement of ocean bottom. *Geophy. Res. Lett*., **23** (8), 861–864 (1996).

Acknowledgments: The research described here was conducted at the Jet Propulsion Laboratory (JPL), California Institute of Technology, under contracts with the National Aeronautics and Space Administration (NASA). We thank Dr. Kejie Chen for providing the seismic inversion data, and Robert Greenwood of Climate & Oceans Support Program in the Pacific (COSPPac), the Australian Bureau of Meteorology, for the tide-gauge data.

Author contributions:

Conceptualization: YTS, JKW

Methodology: PSC, JDMD, SF, YTS

Investigation: YTS, PSC. JDMD, SF, JKW

Visualization: YTS, JDMD

Writing – original draft: YTS

Writing – review & editing: YTS, PSC. JDMD, SF, JKW

Competing interests: Authors declare that they have no competing interests.

Data and materials availability: All data used in this study are publicly available. AltiKa data from https://podaac-opendap.jpl.nasa.gov/opendap/allData/ and SA6 and Jason-3 data from https://podaac.jpl.nasa.gov/dataset/. DART data from https://www.ndbc.noaa.gov/obs.shtml?lat=13&lon=-173&zoom=2&pgm=tsunami. Tide-gauge data from https://www.ioc-sealevelmonitoring.org/ and http://www.bom.gov.au/pacific/. Figures were prepared using Matlab (https://www.mathworks.com/products/matlab.html), a licensed software to JPL.

Supplementary information for

Shocked atmosphere-ocean interplay reveals volcanic tsunami origin and predictive insight

Authors: Y. Tony Song[1*], Philip S. Callahan[1], Jean-Damien M. Desjonqueres[1], Severine Fournier[1] and Josh K. Willis[1]

Affiliations:
[1]Jet Propulsion Laboratory, California Institute of Technology, Pasadena, CA, 91109

*Corresponding author. Email: Tony.Song@jpl.nasa.gov

Supplementary information includes:

Methods
Figs. S1 to S9
References

Methods

Method-1. Computing air-pressure and tsunami initials

We first used seismic data from the USGS website (https://www.usgs.gov/natural-hazards/earthquake-hazards/earthquakes) to determine the precise location of the volcanic eruption and the resulting seafloor deformation. The results are reproducible since seismic data are openly accessible to both the public and tsunami warning systems. Our seismic inversion technique follows the methodology outlined by Chen et al[41,42], yielding a magnitude of Mw5.8 earthquake and a three-dimensional representation of seafloor deformations in the region (Fig. S9). Notably, the inverted seafloor displacements are minimal, only a few centimeters around the crater, with uplift reaching approximately 10 centimeters. This insignificant seafloor deformation discounts the possibility of the destructive Tonga tsunami being caused by the earthquake force alone. Nevertheless, the inversion solution remains valuable for pinpointing the volcanic eruption's location and resultant seafloor deformation.

Subsequently, we utilized the seismic-inverted velocity field (U_s, V_s) of seafloor displacement to establish the initial conditions for our atmosphere and ocean model, respectively. Specifically, we projected the velocity field onto the model grid, and formulated the eruption process by a sinusoidal function, as detailed as follows.

For atmosphere, the initial condition is:

$$(U_A, V_A)(t) = \begin{cases} (U_s, V_s)\ \sin\left(\frac{\pi t}{T}\right)\ E_A, & t \le T \\ 0, & other \end{cases} \quad \text{(S1)}$$

For ocean, the initial condition is:

$$(U_O, V_O)(t) = \begin{cases} -(U_s, V_s)\ \sin\left(\frac{\pi t}{T}\right)\ E_O, & t \le T \\ 0, & other \end{cases} \quad \text{(S2)}$$

In above equations, (U_A, V_A) and (U_O, U_O) represent the depth-averaged air velocity and ocean water velocity, respectively. The variable t denotes time, and T represents the period of an eruption cycle. The positive sign signifies the expulsion of air from the crater, while the negative sign indicates the influx of ocean water towards the crater to fill the cavity created by the eruption.

Analysis of Tonga air-pressure data and satellite imagery reveals three significant eruptions commencing at 4:26, 5:01, and 5:46. Each eruption lasts approximately 20 minutes, with intensity halving over time. Based on this data, we assume a duration of 20 minutes for each eruption cycle; hence, T=120 s. To represent these observations, we applied the initial conditions to the atmosphere and ocean model at each of the eruption commencing times, while reducing the intensity coefficients E_A and E_O by a half each cycle. The initial values of E_A and E_O are determined by fitting the model to the air-pressure data and tsunami measurements, resulting in a value of 0.05 and 0.17, respectively. The head and shoulder pattern of the air pressure (Fig. 1c-e) was reproduced by adding 50% of the E_A and E_O values at the corresponding time step during the initial period of the model.

The resultant energy source (i.e., initially applied to the atmosphere and ocean system) can be calculated in the kinetic energy (KE) form:

$$KE = \frac{1}{2}\rho h \iint (U^2 + V^2)\, dxdy \qquad \text{(S3)}$$

where ρ and h are the density and depth of atmosphere and ocean, respectively. The spatial integral is for the source region, in which *dxdy* is the grid size. The total energy can be obtained by integrating equation (S3) over the eruption period, which has three eruption cycles in the Tonga case. Our calculation yields that the total atmospheric source energy is about 7.8×10^{14} Joule, while the ocean is about 3.5×10^{14} Joule.

The unified initial conditions of equations (S1)-(S3) establish a quantitative relationship between lamb waves and tsunamis within the integrated atmosphere-ocean model. This enables validation through the correlation of air-pressure measurements and tsunami data. Our model domain convers the entire Pacific Ocean, with an average grid size of 3 km, utilizing ETOPO2 for ocean bathymetry. Both lamb waves and tsunamis are barotropic (depth-averaged) long waves. Analysis of air-pressure data from Tonga indicates a wavelength exceeding 40 km, derived from the wave speed of 330 m/s and a cycle period of T=120 s. Such a long wavelength implies that the impact of the eruption extends far beyond the dimensions of the crater.

By comparison, in the 1883 Krakatau case, Nomanbhoy and Satake[43] had an energy estimation of about 2×10^{16} Joule for the tsunami, which is about 58 times of the Tonga case. They assumed an ejecta volume of 270 m in depth and 8 km in diameter. In the Tonga case, the crater size is about 800 m in depth and 4 km in diameter. We can also compare the energy of the Tonga volcanic tsunami to other notable tsunamis for context. For instance, Titov et al[44] and Song[45] estimated a tsunami source energy of 6×10^{15} Joule for the 2004 Sumatra Mw9.1 earthquake, 6.5×10^{14} Joule for the 2010 Chilean Mw 8.8 earthquake, and 3.2×10^{15} Joule for the 2011 Tohoku Mw9.0 earthquake. By comparison, the Tonga volcanic tsunami energy is equivalent to that of a Mw8.0 submarine earthquake.

Method-2. Satellite altimetry

Since the early 1990s, satellite radar altimeters have been providing measurements of sea-level anomaly with accuracy of ~ 1 cm after appropriate corrections[46]. Such an accuracy easily detected the surface displacements (~ 150 cm) of the 2004 Indian Ocean tsunami and the 2011 Japanese tsunami[47,48] but had not observed a volcanic tsunami yet. For volcanic tsunami, the sea surface measurements are different from the ocean bottom pressure,

$$P_b = P_a + \int_{-h}^{\eta} g\rho\, dz \approx P_a + \eta g\rho + \int_{-h}^{0} g\rho\, dz \qquad \text{(S4)}$$

where P_b is total pressure at ocean bottom and P_a is the air pressure at sea surface, while η is the sea-level anomaly being measured by satellite altimeters. At the mean sea level, equation (S4) gives the inverted barometer formulation of $\eta^{ib} = -p_a/g\rho$, where p_a is the air-pressure anomaly. As the air-pressure wave (lamb wave) could not be ignored in the volcanic tsunami, the altimetry measurements should be in the form of $\eta^{A+O} = -\eta^A + \eta^O$, where $\eta^A = p_a/g\rho$ and η^O are the atmospheric and oceanic tsunami, respectively.

For the Tonga volcanic tsunami, we have examined all possible satellite altimetry measurements that might have detected the surface displacement of the tsunamis and identified several passes which had the opportunity to capture the tsunamis (Fig. S7, left). We processed the data to compare with the model by co-locating the satellite passes with the model in time and location. The SARAL/ALtiKa (Satellite with ARgos and ALtiKa), a joint mission between the Indian Space Agency (ISRO) and the French Space Agency (CNES) launched on February 25, 2013, belongs to the global altimetry system for the precise and accurate observations of ocean circulation and sea surface elevation (https://altika-saral.cnes.fr/en/SARAL/GP_mission.htm). Jason-3 and Sentinel-6 Michael Freilich (S6A) are joint missions between NASA, NOAA, EUMETSAT, ESA and CNES. They were launched on January 17, 2016, and November 21, 2020, respectively, with the objective of providing high-precision measurements of global sea-level for climate studies (https://sealevel.jpl.nasa.gov).

We found that the AltiKa satellite captured the near-field tsunami, about 38 minutes after the eruption (Fig. S8a-b), while the S6A and Jason-3 satellites in 30 seconds apart crossed the tsunami through the post-erupted volcano center, 5 hours after the eruption (Fig. S8c-e). We used tsunami travel times to isolate the tsunami signals from ocean dynamic features because altimetry data has both tsunami and ocean dynamic features, while the model only has the tsunami result.

To differ the tsunami signals from ocean dynamic features, we have used a cycle-differentiating method by comparing before and after-cycles of the altimetry passes, as shown in Fig. S7(right, a) for the S6A data as an example. In the ocean between 50°S ~ 60°S large ocean eddies are generated and interact with the fronts of the Antarctic Circumpolar Current, making detection of the tsunami signal difficult. The repeat cycle for these missions is 10 days between successive identical orbits. Because the eddies and fronts in the ocean move slowly over a period of 10 to 20 days[46], while tsunamis travel much faster. This speed difference helps identifying the tsunami fronts. Fig. S7 (right, b) shows the difference around the location of 53°S, where the tsunami propagates according to the travel time, cycle 43 has an abnormal shift in comparison with all prior and subsequent cycles. The difference between cycle 43 and cycle 42 stands out and is consistent with the location and amplitude of the modeled tsunami, confirming detection of the tsunami. Similar results have been obtained for the Jason-3 data, which is not shown here.

Note that AltiKa operated on a drifting cycle and did not follow the same orbit every 10 days; therefore, the cycle-differentiating is ineffective. As a result, the procedure for removing ocean dynamic signals within a 10-day window was not applied to the AltiKa data. This is why significant ocean dynamic signals within a 10-day period remained, as shown in Fig. S8a-b. With the cycle-differentiating, we have processed the S6A and Jason-3 data. The S6A and Jason-3 were on the same pass, but in 30 seconds apart. Fig. S8c-d shows the pass 186 (descending), which was determined over the volcano after 5 hours of the eruption and then observed the tsunami front in the Southern Ocean at latitude of 53°S. Comparing the two satellites data with model (Fig. S8e) shows the agreement of two prominent features: One at the volcano location (~20°S) and the other at the estimated tsunami travel time in the Southern Ocean (~53°S). The high waves at the volcano area suggest the resonance waves were still active after 5 hours of the eruption, while the tsunami front in the Southern Ocean indicates the strength of the tsunami propagating to the southeast direction.

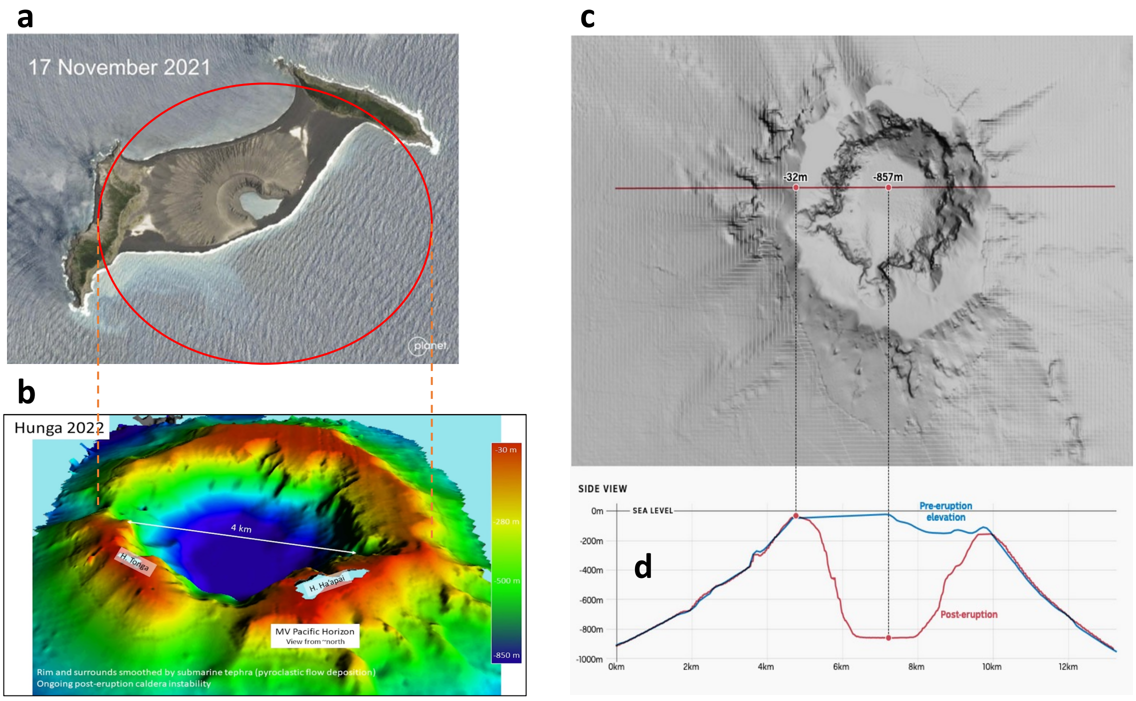

Fig. S1.

Seafloor pre- and post-volcanic eruption on January 15, 2022. a. Satellite image of the HTHH volcano taken on November 17, 2021. **b.** Submarine seafloor survey conducted after the eruption, revealing the volcano's largely intact state with no discernible signs of significant submarine explosions or landslides beyond the volcano. **c.** Top view of the crater. **d.** Side view of the crater before and after the eruption, showing minimal water presence above the volcano before the eruption. Courtesy of Doman et al (2022)[49].

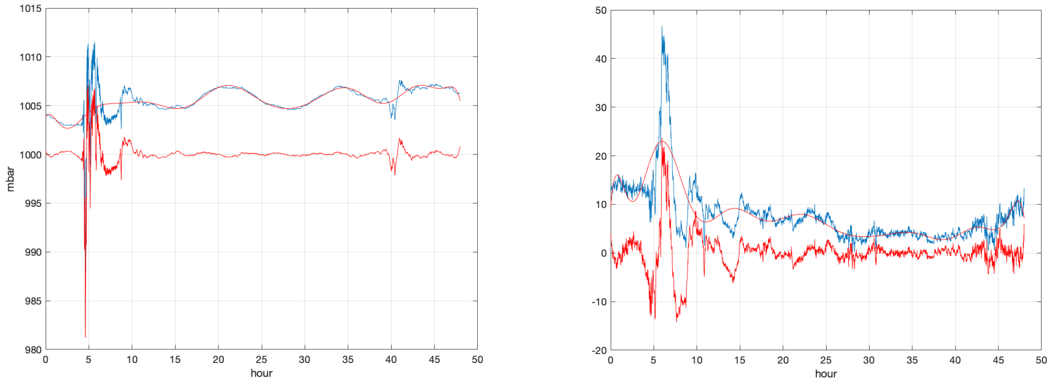

Fig. S2.

Tonga air-pressure (left) and wind (right) data. The blue lines represent the original data, while the red lines represent the mean and the residuals obtained after eliminating the mean oscillations from the data.

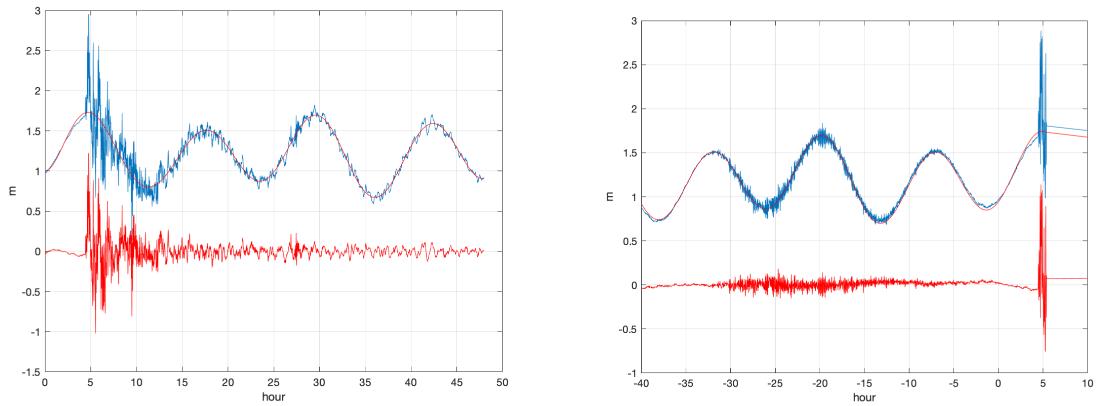

Fig. S3.

Tonga tide-gauges. The two gauges, nkfa2 (on the left) and nkfa (on the right), situated approximately 1.8 km apart, at longitude of 175.1967°W and latitude of 21.1303°S. The blue lines depict the original data, whereas the red lines illustrate the mean values and the residuals obtained following the removal of the mean tidal components from the data. It's noteworthy that the nkfa tide-gauge malfunctioned after 5:25 UTC. Pre-eruption data were used to compute the mean tides.

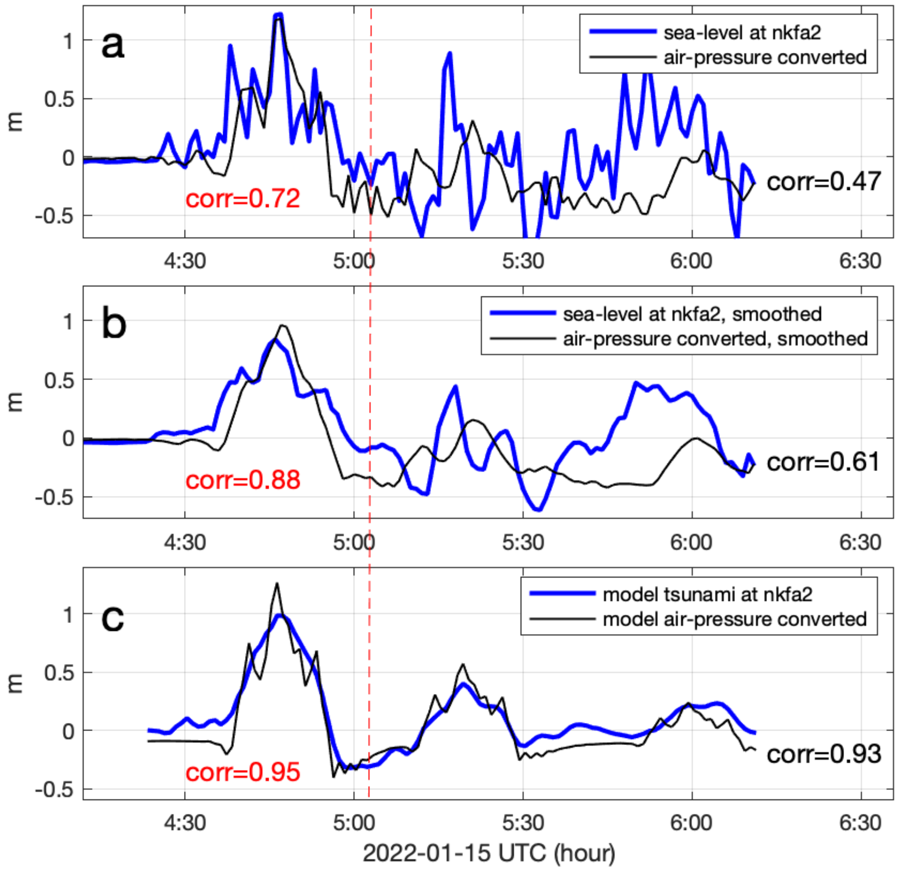

Fig. S4.

Correlation values: (with a confidence interval exceeding 99.9%) between Tonga tide-gauge data at nkfa2 (on the left) and air-pressure data converted into sea-level by equations (1)-(2). **a**. the original data, **b.** the smoothed data, and **c.** the corresponding model results. The correlation values are color-coded as follows: (red) for the first-wave period and (black) for the entire period.

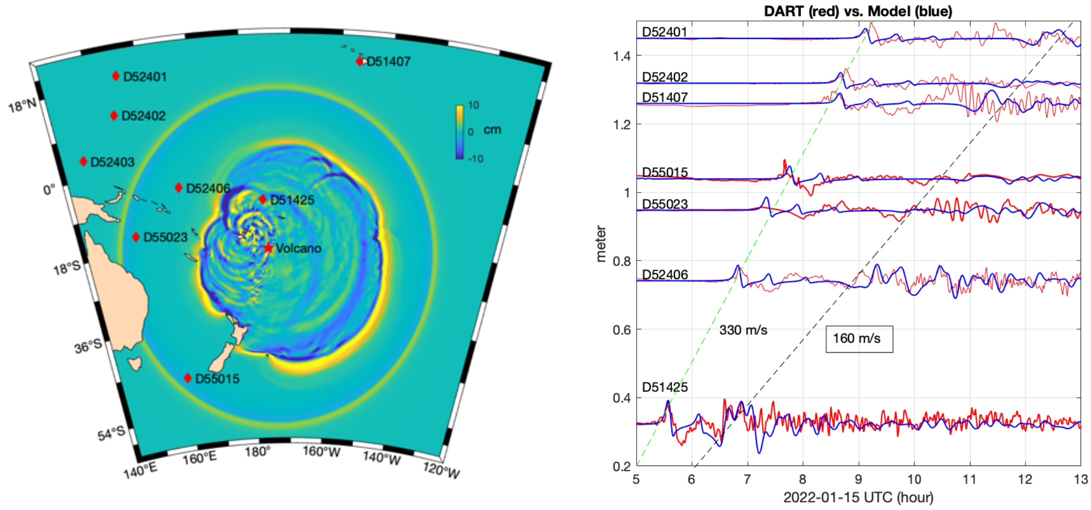

Fig. S5.

Validation by DART data. (left) DART locations and modeled ocean bottom pressure. (right) Comparison with DART measurements at each location. The green and dark dash-lines represent the lamb wave speed (330 m/s) and the averaged oceanic tsunami speed (160 m/s), respectively.

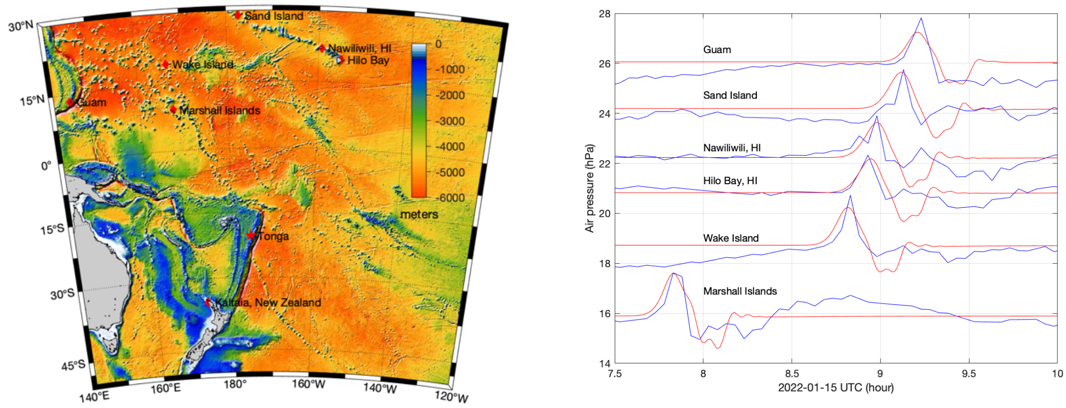

Fig. S6.

Validation by far-field air-pressure data. (left) Air-pressure sensor locations on the topography map. (right) Comparison with air-pressure measurements at each location, blue for data and red for model. Note that the air-pressure waves start with a low anomaly center, then propagate into high anomaly in the far fields. See Lynett et al (2022, Extended Data Fig. 4) for more details.

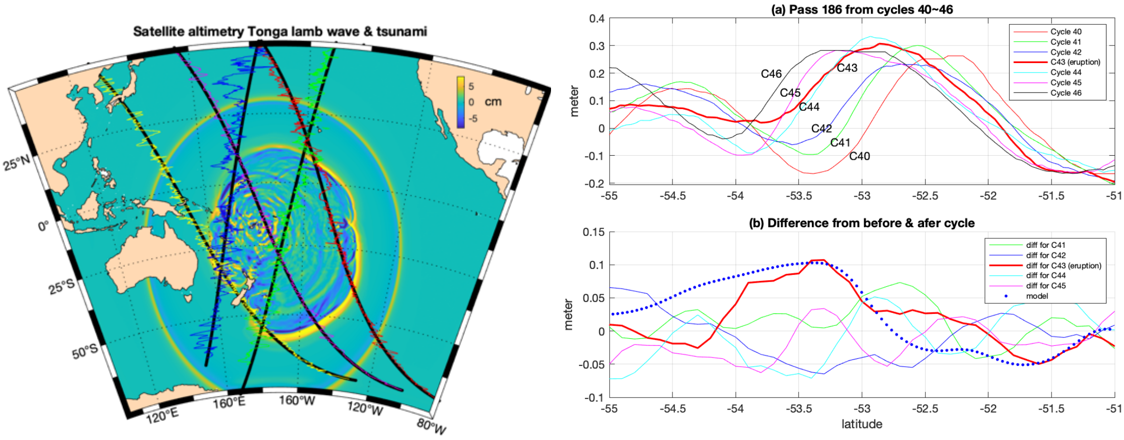

Fig. S7.

Satellite altimetry. (left) Satellite altimetry passes on the map of the tsunami. (right) Process for isolating the tsunami signal: (a) Extracting the sea-surface height anomaly (SSHA) from S6A altimetry data during cycles surrounding the eruption cycle, and (b) Removal of cycles before and after the eruption cycle. The blue dotted line represents the model tsunami, which aligns with the isolated satellite data.

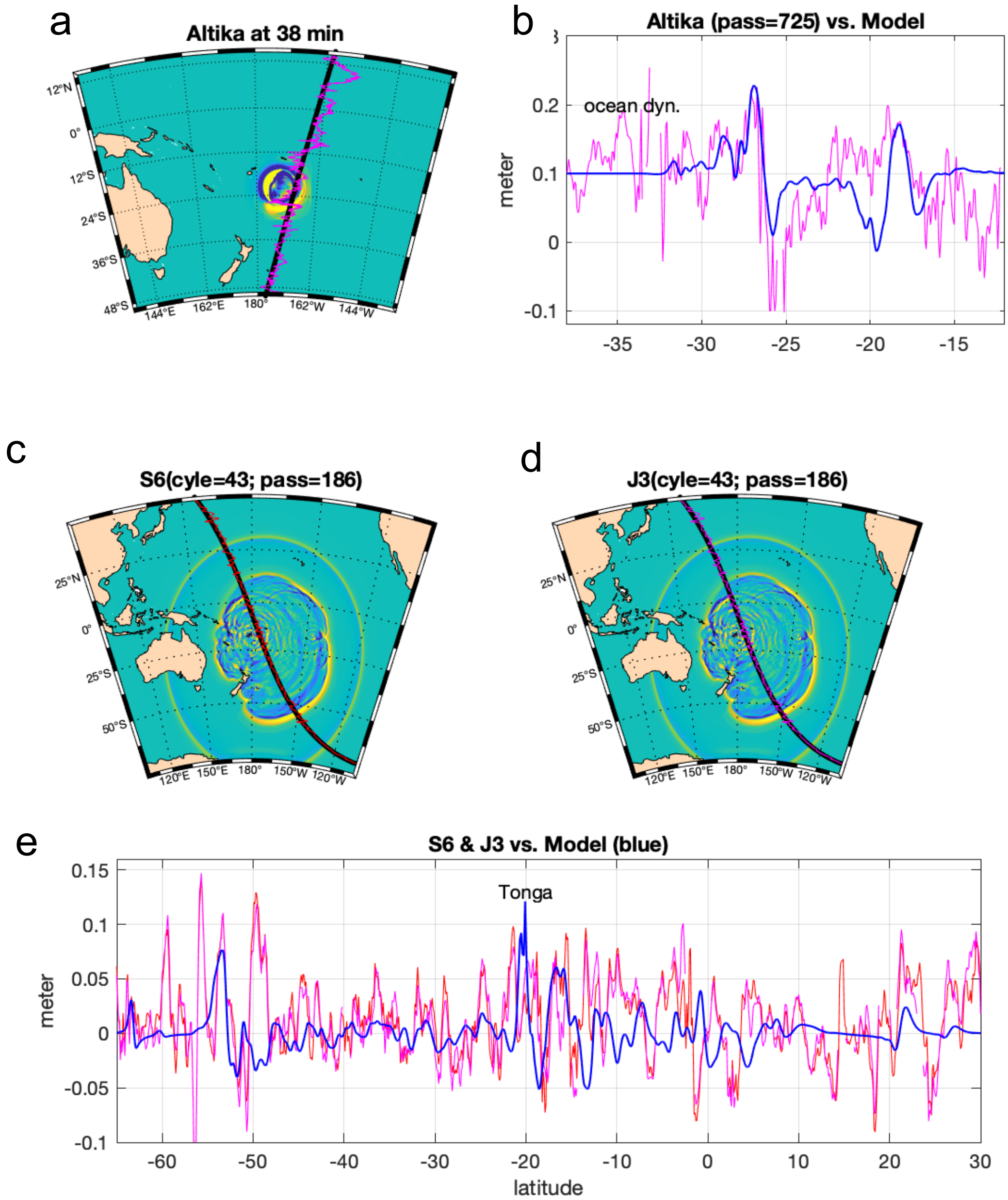

Fig. S8. Satellite altimetry and model comparison. a. AltiKa satellite pass. **b.** Comparison between altimetry sea-level (magenta) and the model (blue). **c.** S6A satellite pass. **d**. Jason-3 satellite pass. **e**. Comparison between altimetry sea-level (magenta and red) and the model (blue). Note that the tsunami amplitude is well within the range of ocean dynamic signals, suggesting that the tsunami had quickly diminished about 40 minutes after the eruption.

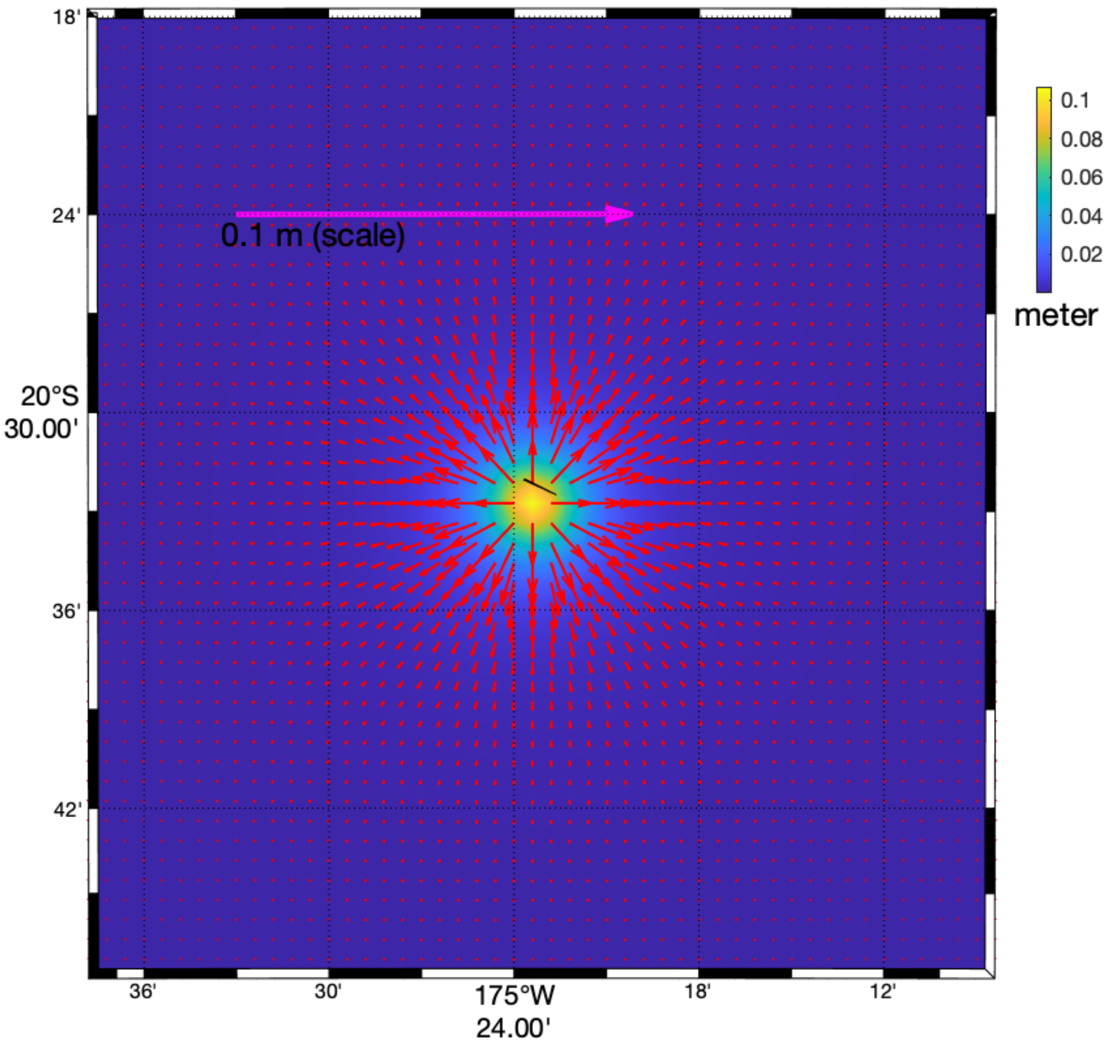

Fig. S9.

Seafloor displacement of the Tonga volcanic eruption inverted from seismic data. Arrows represent the horizontal displacement, while the background color is the vertical displacement.

References

41. K. Chen, Liu Z., Y. T. Song , Automated GNSS and teleseismic earthquake inversion (AutoQuake Inversion) for tsunami early warning: retrospective and real-time results, *PAAG*, (2019a). DOI: 10.1007/s00024-019-02252-x.
42. K. Chen, J. Smith, J. Avouac, Z. Liu Z., Y. T. Song, G. Adriano, Triggering of the Mw 7.2 Hawaii earthquake of May 4, 2018 by a dike intrusion. *Geophysical Research Letters,* (2019b). doi: https://doi.org/10.1029/2018GL081428**.**
43. N. Nomanbhoy, K. Satake, Generation mechanism of tsunamis from the 1883 Krakatau eruption, *Geophys. Res. Letters*, **22**, 509-512 (1995).
44. V. Titov, Y. T. Song, L. Tang, E. N. Bernard, Y. Bar-Sever, Y. Wei, Consistent estimates of tsunami energy show promise for improved early warning, *Pur Appl. Geophs*., (2016). doi: 10.1007/s00024-016-1312-1.
45. Y. T. Song, Detecting tsunami genesis and scales directly from coastal GPS stations, *Geophys. Res. Lett*., **34** (2007). https://doi.org/10.1029/2007GL031681.
46. L.-L. Fu, Pattern and velocity of propagation of the global ocean eddy variability, *J. Geophys. Res. – Oceans*, **114**, C11017, (2009). doi:10.1029/2009JC005349.
47. Song, Y. T., C. Ji, L.-L. Fu, V. Zlotnicki, C.K. Shum, Y. Yi, and V. Hjorleifsdottir The 26 December 2004 Tsunami Source Estimated from Satellite Radar Altimetry and Seismic Waves, *Geophys. Res. Lett*., **23** (2005). doi:10.1029/2005GL023683.
48. Song, Y. T., I. Fukumori, C.K. Shum, and Yuchan Yi, Merging tsunamis of the 2011 Tohoku-Oki earthquake detected over the open ocean, *Geophys. Res. Lett*., (2012). doi:10.1029/2011GL050767.
49. D. Doman, A. Palmer, The 'mind-blowing' sea floor changes caused by Tongan volcanic eruption (2022). https://www.abc.net.au/news/2022-11-21/sea-floor-map-reveals-huge-cavity-left-behind-by-tonga-volcano/101674708.

We thank the reviewers for their time spent reviewing this manuscript and for their insightful comments, which have greatly improved the manuscript. We have responded to their comments item-by-item in bold and italicized text. We have also submitted an in-line track-changes version of the revised manuscript and a response to the annotated PDF, with corresponding text additions and line numbers indicated.

Specifically, we have revised the manuscript in three major areas:

1. **As suggested by the reviewer, we have changed the title to reflect the novel contributions from the HTHH case study. The new title is "Coupled atmosphere-ocean source mechanism reveals predictors of the 2022 Tonga volcanic tsunami."**
2. **The main text and Supplementary Information have been thoroughly revised. All reviewers' comments have been considered and addressed.**
3. **Figure 4 has been updated with additional evidence from co-located measurements of an air-pressure sensor and tide gauge at Fiji Suva, further strengthening our conclusions.**

We believe the reviewers' feedback has made this manuscript clearer, more robust, and overall better.

Response to Reviewer Comments in bold and italic.

Reviewer #1 (Remarks to the Author):

The authors investigated the 2022 Hunga Tonga – Hinga Ha'apai tsunami resulting from the interaction between the air pressure created by the eruption and the ocean, by using an integrated ocean-atmosphere model. The results were validated from tide gauges, pressure gauges and satellite altimetry. I think the work has potential to be considered for publication, however, there are several major concerns that need to be addressed. The main points are reported below:

We thank Reviewer #1, Dr Andrea Verolino, for recognizing the potential of this study.

Major points:
• The title seems to be general in nature and potentially applicable to all volcanoes in similar shallow settings, however, the work proposed here only refers to HTHH and vaguely to Krakatau, with no further tests on other volcanoes. It should be reflected in the tile that was only for one case study: HTHH.

We agree. The title has been changed to: Coupled atmosphere-ocean source mechanism reveals predictors of the 2022 Tonga volcanic tsunami.

• The rationale behind the inclusion of some text on the 2018 Krakatau event is not clear nor contextualised. Was that event also entirely resulting from air-ocean interactions? It is not really investigated in the paper and seems out of context. If the intent of the authors was to argue that the 2018 Krakatau tsunami had a completely different origin mechanism than previously hypothesised, then at the moment it has just a speculative nature.

We agree with the point to focus on the HTHH in this work, so we have deleted the discussion of the 2018 Ana Krakatau event. We also believe that many historical volcanic tsunamis should be re-examined after the surprised evidence of the 2022 Tonga event, which clearly contradicts to previous assumptions. We have cited the review paper of Schindele et al (2024) to encourage future studies on volcanic tsunami genesis.

• Some of the parameters used for the model (crater diameter and crater depth) are approximative and retrieved (from my understanding) from a newspaper article (https://www.abc.net.au/news/2022-11-21/sea-floor-map-reveals-huge-cavity-left-behind-by-tonga-volcano/101674708). Research articles should be used for this purpose.

Yes, research articles and data source have been cited:
Mackay, K. Digital elevation models of Hunga Volcano; pre- and post- 15 January 2022 eruption. Zenodo https://doi.org/10.5281/zenodo.7456324 (2022). Mével, L., H., Miller, C. A., Ribó, M., Cronin, S., & Kula, T. (2023). The magmatic system under Hunga volcano before and after the 15 January 2022 eruption. Science Advances, 9(50), eadh3156.

• The model shown in fig. 2 should be explained more clearly. There are several points that made me raise some questions (see various comments in the annotated pdf).

Figure 2 has been revised to clarify the parameters and methods used in the calculation. To keep the page-limit, we added sufficient details in the Supplementary Information (Method 2).

• The discussions lack any possible contribution, even if minor, of other tsunami source mechanisms. For example, the bathymetry they use shows clear landsliding from the rim within the caldera (Fig. S1).

We agree and thank you for the useful suggestions. We have two major revisions:

1. ***We obtained more supporting evidence from the co-located air-pressure and tide-gauge measurements from Fiji Suva location. Figure 4 is completely re-produced to clarify the prediction skills on volcanic tsunamis in near-field.***
2. ***We added a paragraph to emphasize the contributions of this study:***

"Thanks to the unprecedented observational evidence from the recent Tonga incident, our study offers two innovative contributions: A) The coupled atmosphere-ocean source mechanism provides a unified explanation for the mysterious formations of air-pressure waves and volcanic tsunamis, enabling a re-examination of previous assumptions about historical events. B) The predictive potential of the leading air-pressure waves for destructive tsunamis holds practical value. Our predictive formula, based on simple equations (1)-(2) and inexpensive air-pressure sensors, represents the first step toward a practical early warning system for volcanic tsunamis."

See annotated pdf for minor and major comments in detail.
Dr Andrea Verolino

Thank you very much for the annotated comments. They are insightful and constructive. We have considered them all in the revised version. For your information, we have also submitted the response file to the annotated pdf.

Reviewer #2 (Remarks to the Author):

Recommendation to the manuscript background information
Certainly! Here are some suggestions for revising the background information section of the manuscript.

We thank Reviewer #2 for the constructive suggestions. We have revised the manuscript substantially with three major improvements:

A. ***We changed the title to reflect the main subject of the study***
B. ***We revised the main text and Supplementary Information thoroughly***
C. ***We provided additional evidence from co-located measurements of air-pressure sensor and tide-gauge at Fiji Suva to support our conclusions. Figure 4 have been improved with additional data.***

Our item-by-item responses are the following:

1. Contextual Framework: Provide a concise overview of the current state of knowledge regarding volcanic tsunamis, highlighting key challenges and gaps in understanding the mechanisms that trigger volcanic tsunamis. Emphasize the difficulty in accurately predicting their occurrence and impact on coastal communities.

Thanks for the suggestion. We have revised the introduction section with a concise overview of the current state of knowledge. We also cited a review paper on the volcanic tsunami of Schindele et al (2024), which is very helpful.

2. Historical Perspective: Briefly discuss significant historical events involving volcanic tsunamis, such as documented cases and their impact, including the Krakatau eruption of 1883 and more recent incidents (2018 Anak Krakatau, Pakoksung et al, 2019), to illustrate the destructive potential and variability of volcanic tsunamis.

Yes, we included the historical perspective of source mechanisms for volcanic tsunamis. We briefly discussed previous studies on the HTHH:
"Omira et al[21] and Ren et al[22] demonstrated the atmospheric origin of the tsunami by simulating the Proudman resonance effect of air-pressure waves over deep-ocean trenches. Pakoksung et al[23] and Purkis et al[24] simulated the tsunami by the submarine explosion scenario without the atmospheric effect. Their simulations involved either a single explosion of 25 megatons or three increasingly larger explosions of 0.5, 4, and 15 megatons, respectively. In contrast, Lynett et al[25] suggested multiple mechanisms for the tsunami by prescribing the air-pressure and tsunami initial conditions separately."

3. Novel Research Question or Hypothesis: Clearly state the specific research question or hypothesis that your study is addressing. Explain how this query

addresses a gap in the current understanding of volcanic tsunami mechanisms or predictive capabilities.

We expanded the introduction to include our novel research and science hypothesis:

"The central question is how the volcanic eruption managed to trigger such a destructive tsunami with a relatively small amount of water present. Despite the discovery of the Lamb wave over a century ago in 1881, its connection to volcanic tsunamis at the source region remains elusive.

These uncertainties surrounding the genesis of tsunamis and air-pressure waves underscore the challenges in predicting volcanic tsunamis effectively to safeguard lives. In this study, we found an intrinsic coupling between air-pressure waves and tsunamis at the source region during their formation. Using an integrated atmosphere-ocean model, we show that this coupling originates from the volcanic ejection process, which causes lateral explosions of air to form air-pressure waves and a proportional influx of water in the ocean to trigger tsunamis. Since the volcanic ejecta results from the mass loss in the ocean, the principle of mass conservation allows the fast-moving air-pressure waves to provide predictive insights for tsunamis. This coupled atmosphere-ocean source mechanism is distinct from previously proposed mechanisms, offering a novel understanding of volcanic tsunami genesis and potential for early warning systems in the near field, where most fatalities occur."

4. Unique Methodological Approach: Describe the innovative methodology or approach utilized in the study, such as the integration of an atmosphere-ocean model, a unique use of satellite altimetry data, or a creative application of air-pressure sensors for tsunami prediction.

We detailed the Method in the Supplementary, including deriving the kinetic energy and potential energy, and initial conditions for the atmosphere and ocean models using the observed crater volume and parameters.

We emphasized our unique approach in the Abstract:
"We constructed an integrated atmosphere-ocean model to explain the underlying mechanism and validated it with various data, including, for the first time, satellite altimetry measurements."

5. Prior Research: Summarize previous studies and hypotheses related to volcanic tsunami generation mechanisms. Mention existing models or theories (without going into excessive detail) to provide context for how your study builds upon or challenges these previous findings.

Yes, we included a summary:
Previous studies have suggested at least eight formation mechanisms[17-20]. These include the subaerial landslides, submarine landslides, pyroclastic flows, caldera

or flank collapses, collapses of eruptive column, deep-ocean explosions, volcano-tectonic earthquakes, and the atmospheric origin of air-pressure waves.

6. Importance of Air-Pressure Waves: Introduce air-pressure waves, such as the "lamb wave," in understanding volcanic tsunami dynamics. Discuss the importance of studying air-pressure waves for enhancing early warning systems and disaster preparedness strategies.

Excellent suggestions. We added paragraphs:
"We found that the air-pressure waves can predict tsunamis with lead times of 5 minutes, 10 minutes, and 50 minutes at distances of 30 km, 65 km (Tonga), and 280 km (Fiji – Suva) from HTHH, respectively."
"Based on the Tonga data and post-event surveys[9,26], a volcanic air-pressure anomaly exceeding 15 mbar could indicate an impending destructive tsunami, as marked by the magenta dotted lines in Fig. 4 (b) and 4(-c). This suggests that air-pressure sensors could be employed for volcanic tsunami early warning."

7. Study Objectives: Clearly outline the study objectives in the background section to guide readers and manage expectations, such as discovering new predictors or enhancing predictive models for volcanic tsunamis.

We included the suggested revision by adding:
"Given the observational evidence and model demonstrations from the 2022 Tonga volcanic incident, it is strongly recommended to deploy air pressure sensors across coastal communities surrounding potentially tsunamigenic volcanoes, about ninety worldwide[17]. Air-pressure sensors are inexpensive to install and have traditionally been maintained by weather forecasting agencies, which are also responsible for tsunami early warning."

8. Transition to Methodology: Transition smoothly from the background section to the methodology section by explaining how your study addresses gaps identified in prior research. This can help justify the need for your chosen methodology and research approach.

Yes, we added details in the Supplementary Information on the source mechanism and parameters used in estimating the tsunami energy. We included:

The tsunami source energy also can be estimated by the crater volume. From observational data, we determine that the crater has a diameter of 4 km and a depth of 800 m, resulting in a volume of approximately $\pi r^2 D \approx 10$ km^3, where r = 2 km and D = 0.8 km. This volume of water must be displaced from around the volcano to the crater by influxes of water, represented by the flow field (U_O,V_O) in equation (S2). This influx would cause a mass loss of water from a larger circular

area A=πR^2, resulting in a sea-level depression of η around the volcano. The resultant potential energy (PE) is:

$$PE = \frac{1}{2}\rho g \eta^2 A. \qquad (S4)$$

9. Conciseness and Focus: Keep the background section concise and focused, avoiding unnecessary details or tangential information that may distract from the manuscript's main objectives.

Yes, we added more details in the Supplementary with necessary materials to keep the man text concise and informative.

By revising the background information in this manner, you can provide a clear and informative context for your study on volcanic tsunamis. This will ensure that readers understand the significance of your research within the broader field of natural hazards and tsunami science.

In the conclusive section, we summarized our main contribution and objectives of this study:

"our study offers two innovative contributions: A) The coupled atmosphere-ocean source mechanism provides a unified explanation for the mysterious formations of air-pressure waves and volcanic tsunamis, enabling a re-examination of previous assumptions about historical events. B) The predictive potential of the leading air-pressure waves for destructive tsunamis holds practical value. Our predictive formula, based on simple equations (1)-(2) and inexpensive air-pressure sensors, represents the first step toward a practical early warning system for volcanic tsunamis.